Pyramidal surface textures for light trapping and antireflection in perovskite-on-silicon tandem solar cells

Bennett W. Schneider,[1] Niraj N. Lal,[1] Simeon Baker-Finch,[1,2] and Thomas P. White[1,*]

[1] *Centre for Sustainable Energy Systems, Research School of Engineering, Australian National University, Canberra 0200, Australia.*
[2] *PV Lighthouse, Coledale, NSW 2515, Australia.*

[*] *thomas.white@anu.edu.au*

Abstract: Perovskite-on-silicon tandem solar cells show potential to reach $>30\%$ conversion efficiency, but require careful optical control. We introduce here an effective light-management scheme based on the established pyramidal texturing of crystalline silicon cells. Calculations show that conformal deposition of a thin film perovskite solar cell directly onto the textured front surface of a high efficiency silicon cell can yield front surface reflection losses as low as $0.52\,\mathrm{mA/cm^2}$. Combining this with a wavelength-selective intermediate reflector between the cells additionally provides effective light-trapping in the high-bandgap top cell, resulting in calculated absolute efficiency gains of $2-4\%$. This approach provides a practical and effective method to adapt existing high efficiency silicon cell designs for use in tandem cells, with conversion efficiencies approaching 35%.

OCIS codes: (350.6050) Solar energy; (310.4165) Multilayer design; (310.1210) Antireflection coatings; (230.1480) Bragg reflectors.

References and links

1. K. Masuko, M. Shigematsu, T. Hashiguchi, D. Fujishima, M. Kai, N. Yoshimura, T. Yamaguchi, Y. Ichihashi, T. Yamanishi, T. Takahama, M. Taguchi, E. Maruyama, and S. Okamoto, "Achievement of more than 25% conversion efficiency with crystalline silicon heterojunction solar cell," presented at the 40th IEEE Photovoltaics Specialist Conference (PVSC), Denver, USA, 8–13 June 2014.
2. M. A. Green, "Third generation photovoltaics: Ultra-high conversion efficiency at low cost," Prog. Photovoltaics: Res. Appl. **9**(2), 123-135 (2001).
3. H. Snaith, "Perovskites: the emergence of a new era for low-cost, high-efficiency solar cells," J. Phys. Chem. Lett. **4**, 3623–3630 (2013).
4. J. Burschka, N. Pellet, S.-J. Moon, R. Humphry-Baker, P. Gao, M. K. Nazeeruddin, and M. Grätzel, "Sequential deposition as a route to high-performance perovskite-sensitized solar cells," Nature **499**, 316–319 (2013).
5. M. Liu, M. B. Johnston, and H. J. Snaith, "Efficient planar heterojunction perovskite solar cells by vapour deposition," Nature **501**, 395–399 (2013).
6. T. P. White, N. N. Lal, and K. R. Catchpole, Tandem solar cells based on high-Efficiency c-Si bottom cells: top cell requirements for $>30\%$ efficiency, IEEE J. Photovoltaics **4**(1), 208–214 (2014).
7. N. N. Lal, T. P. White, and K. R. Catchpole, "Optics and light-trapping for tandem solar cells on silicon," IEEE J. Photovoltaics (to be published).
8. S. Baker-Finch and K. McIntosh, "Reflection of normally incident light from silicon solar cells with pyramidal texture," Prog. Photovoltaics: Res. Appl. **19**(4), 406–416 (2011).
9. S. J. Kim, G. Y. Margulis, S. B. Rim, M. L. Brongersma, M. D. McGehee, and P. Peumans, "Geometric light trapping with a V-trap for efficient organic solar cells," Opt. Express **21**(S3), A305–A312 (2013).

#216827 - $15.00 USD Received 11 Jul 2014; revised 4 Aug 2014; accepted 17 Aug 2014; published 28 Aug 2014

10. M. M. de Jong, P. J. Sonneveld, J. Baggerman, C. J. M. van Rijn, J. K. Rath, and R. E. I. Schropp, "Utilization of geometric light trapping in thin film silicon solar cells: simulations and experiments," Prog.Photovolt: Res. Appl. **22**(5), 540–547 (2014).
11. S. B. Rim, S. Zhao, S. R. Scully, M. D. McGehee, and P. Peumans, "An effective light trapping configuration for thin-film solar cells," Appl. Phys. Lett. **91**, 243501 (2007).
12. G. Li, H. Li, J. Y. L. Ho, M. Wong, and H. S. Kwok, "Nanopyramid structure for ultrathin cSi tandem solar cells," Nano Letters **14**(5), 2563–2568 (2014).
13. D. Dominé, P. Buehlmann, J. Bailat, A. Billet, A. Feltrin, and C. Ballif, "Optical management in high-efficiency thin-film silicon micromorph solar cells with a silicon oxide based intermediate reflector," Phys. Stat. Solidi **2**(4), 163–165 (2008).
14. S. Fahr, C. Rockstuhl, and F. Lederer, "Metallic nanoparticles as intermediate reflectors in tandem solar cells," Appl. Phys. Lett. **95**, 121105 (2009).
15. S. Fahr, C. Rockstuhl, and F. Lederer, "The interplay of intermediate reflectors and randomly textured surfaces in tandem solar cells," Appl. Phys. Lett. **97**, 173510 (2010).
16. P. G. O'Brien, A. Chutinan, K. Leong, N. P. Kherani, G. A. Ozin, and S. Zukotynski, "Photonic crystal intermediate reflectors for micromorph solar cells: a comparative study," Opt. Express **18**(5), 4478–4490 (2010).
17. S. Fahr, C. Rockstuhl, and F. Lederer, "Sandwiching intermediate reflectors in tandem solar cells for improved photon management," Appl. Phys. Lett. **101**, 133904 (2012).
18. P. G. O'Brien, Y. Yang, A. Chutinan, P. Mahtani, K. Leong, D. P. Puzzo, L. D. Bonifacio, C.-W. Lin, G. A. Ozin, and N. P. Kherani, "Selectively transparent and conducting photonic crystal solar spectrum splitters made of alternating sputtered indium-tin oxide and spin-coated silica nanoparticle layers for enhanced photovoltaics," Sol. Energy Mater. Sol. Cells **102**, 173–183 (2012).
19. J. G. Mutitu, S. Shi, C. Chen, T. Creazzo, A. Barnett, C. Honsberg, and D. W. Prather, "Thin film silicon solar cell design based on photonic crystal and diffractive grating structures," Opt. Express **16**(19), 15238–15248 (2008).
20. S. Sun, T. Salim, N. Mathews, M. Duchamp, C. Boothroyd, G. Xing, T. C. Sum, and Y. M. Lam, "The origin of high efficiency in low-temperature solution-processable bilayer organometal halide hybrid solar cells," Energy Environ. Sci. **7**, 399–407 (2014).
21. S. De Wolf, J. Holovsky, S-J. Moon, P. Lo*p*er, B. Niesen, M. Ledinsky, F-J. Haug, J-H. Yum, and C. Ballif, "Organometallic halide perovskites: sharp optical absorption edge and its relation to photovoltaic performance," J. Phys. Chem. Lett. **5**(6), 1035–1039 (2014).
22. A. Martí and G. Araújo, "Limiting efficiencies for photovoltaic energy conversion in multigap systems," Sol. Energy Mater. Sol. Cells **43**, 203–222 (1996).
23. G. E. Eperon, S. D. Stranks, C. Menelaou, M. B. Johnston, L. M. Herz, and H. J. Snaith, "Formamidinium lead trihalide: a broadly tunable perovskite for efficient planar heterojunction solar cells," Energy Environ. Sci. **7**, 982–988 (2014).
24. Z. Zhao, A.Wang, M. A. Green, and F. Ferrazza, "19.8% efficient "honeycomb" textured multicrystalline and 24.4% monocrystalline silicon solar cells," Appl. Phys. Lett. **73**, 1991–1993 (1998).
25. M. A. Green, "The path to 25% silicon solar cell efficiency: history of silicon cell evolution," Prog. Photovoltaics: Res. Appl. **17**(3), 183–189 (2009).
26. M. A. Green, K. Emery, Y. Hishikawa, and W. Warta, "Solar cell efficiency tables (version 36)," Progress in Photovolt: Res. Appl. **18**(5), 346–352 (2010).
27. PV Lighthouse, OPAL 2, 2011. [Online]. http://www.pvlighthouse.com.au/calculators/OPAL 2/OPAL 2.aspx.
28. Orfanidis, Electromagnetics Waves and Antennas, http://www.ece.rutgers.edu/ orfanidi/ewa/ retrieved June 2013.
29. F. Deschler, M. Price, S. Pathak, L. Klintberg, D. D. Jarausch, R. Higler, S. Huettner, T. Leijtens, S. D. Stranks, H. J. Snaith, M. Atature, R. T. Phillips, and R. H. Friend, "High photoluminescence efficiency and optically pumped lasing in solution-processed mixed halide perovskite semiconductors," J. Phys. Chem. Lett. **5**(8), 1421–1426 (2014).

1. Introduction

Crystalline silicon cells dominate the current photovoltaic market. While the record efficiency of these cells recently passed 25% [1], long term goals of achieving efficiencies $> 30\%$ in silicon-based technologies must overcome the theoretical efficiency limits of single-junction cells [2]. Recent developments in thin-film solar cells [3–5] are driving interest in tandem cells that combine low-cost thin-film technology with current high-efficiency crystalline silicon (c-Si) cells. This approach has the potential to achieve efficiencies above 30% while taking full advantage of established c-Si cell manufacturing capabilities [3, 6, 7].

There are three critical optical requirements for this approach:

1. Low front-surface reflectance;

#216827 - $15.00 USD Received 11 Jul 2014; revised 4 Aug 2014; accepted 17 Aug 2014; published 28 Aug 2014

2. Selective light trapping in the top cell; and

3. High transmission of sub-bandgap light through the top cell.

Requirement 1 is critical to achieve high conversion efficiencies in any solar cell, while the importance of requirements 2 and 3 depends on the relative absorption and carrier transport properties of the thin-film top cell.

Here we propose a tandem cell geometry as illustrated in Fig. 1 in which the thin-film top cell is deposited conformally onto a pyramidally-textured c-Si cell that incorporates an intermediate Bragg reflector between the cells. This geometry retains the excellent anti-reflection properties of the original silicon cell while providing wavelength-selective light trapping in the top cell. We show that the combination of an optimized single-layer anti reflection coating (SLARC) and Bragg reflector can provide a 20% increase in short circuit current in a 200 nm thick top cell, and almost double the short circuit current in a 50 nm thick top cell, compared to a planar tandem cell with a SLARC. Applying these results to a simple tandem cell efficiency model for a perovskite-on-silicon tandem, we estimate that the combined texture and Bragg reflector design can yield absolute efficiency gains of $2-4\%$ compared to a planar tandem cell.

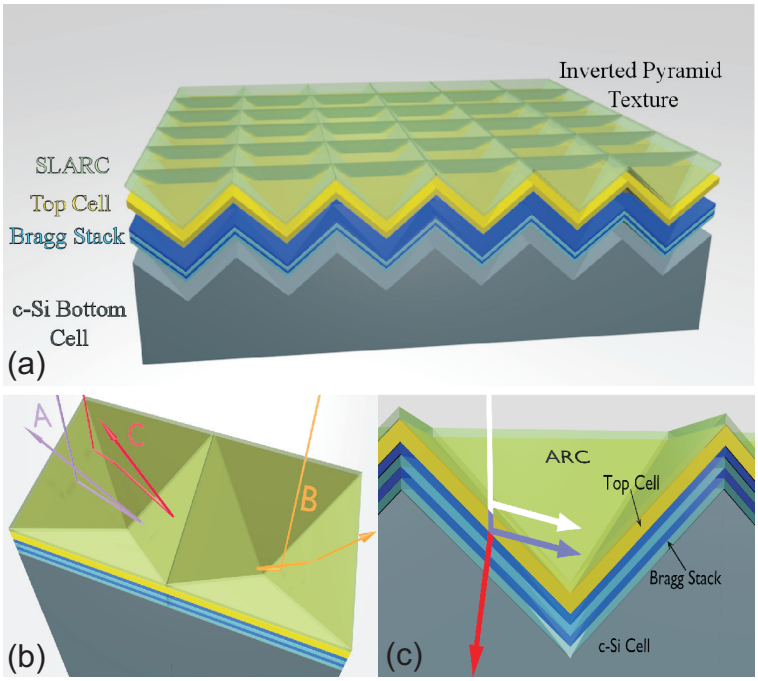

Fig. 1. (a) Wide-angle view of textured surface showing conformal deposition of layers in cross-section. (b) Three possible light paths for inverted pyramid texture [8]. (c) Schematic cross-section of internal optical structure: the intermediate reflector transmits low-energy light (red arrow) into the bottom c-Si cell, and reflects short wavelength light (indigo arrow) back into the top cell.

2. Macro-scale surface textures and light trapping in tandem cells

Conventional monocrystalline c-Si cells achieve excellent anti-reflection properties ($< 1\%$ across the solar spectrum) through a combination of a dielectric anti-reflection coating and pyramidal surface texturing defined by the $[111]$ crystallographic planes of Si. Low reflectance

#216827 - $15.00 USD Received 11 Jul 2014; revised 4 Aug 2014; accepted 17 Aug 2014; published 28 Aug 2014

occurs due to multiple reflections from the pyramidal surfaces as illustrated in Fig. 1. Similar textures have also been used for light trapping in thin film cells by depositing the absorbing layer onto pyramidal or v-groove textured substrates [9–11]. In a recent work by Li *et al.*, a 300 nm a-Si cell was conformally deposited onto an 8 µm thick c-Si cell patterned with inverse pyramids to create an α-Si/c-Si tandem [12]. The texturing provided broadband anti-reflection at short wavelengths, while some light trapping was observed in the top cell due to diffraction effects from the 1 µm period pyramid array.

Achieving simultaneous trapping of short wavelength light in the top cell and transmission of long wavelength light to the bottom cell (requirements 2 and 3 above) is a major challenge for tandems. Broadband scattering of light back into the top cell is detrimental since long wavelength light is lost through the front of the cell [7]. Thus, a wavelength-selective intermediate reflector is required to maximize the light-trapping benefits of a textured surface. A large body of work has been published on light-trapping in micromorph Si cells (a thin-film tandem of α-Si:H and µc-Si:H), which are typically deposited onto textured substrates with sub-wavelength features [13–18]. Combining a selective intermediate reflector (IR) with these surfaces can provide significant light-trapping in the top cell. Various types of IRs have been studied, including 1D, 2D and 3D photonic crystals [15–19] and metallic nanoparticles [14].

We propose here an approach that combines elements of both schemes described above; namely a thin film top cell deposited conformally onto a macro-scale textured bottom cell, with a wavelength-selective intermediate reflector between the two cells. In this way, we exploit simultaneously the excellent anti-reflection properties of pyramidally-textured silicon, and the geometric light trapping provided by an increased path length for short wavelength light in the top cell (Fig. 1).

3. Cell structure and optical model

We model the optical properties of the tandem cell using the simplified geometry shown in Fig. 1. The untextured (planar) cell is modeled as a multilayer stack using a simple transfer matrix method. For the textured cases, we apply the semi-analytic method described in [8] which takes into account the different ray paths and angles of incidence for light incident on the pyramidal surface (Fig. 1(b)). The polarization-dependent reflection and transmission coefficients are calculated using the same transfer matrix code.

The top cell is treated as a single absorbing layer with a thickness between 50 nm and 250 nm, typical of current perovskite cells [3, 20]. The absorbing layer is taken to have a refractive index of 3, and wavelength-dependent absorption of a direct-bandgap semiconductor with characteristic absorption coefficient $\alpha_0 = 2 \times 10^4\,\mathrm{cm}^{-1}$, chosen by fitting a direct-bandgap absorption model [6] to the perovskite absorption coefficient data in [21]. The top cell bandgap is set at $E_{g,top} = 1.7\,\mathrm{eV}$: the optimum bandgap for a dual junction tandem with c-Si [22]. This bandgap is larger than the most common $CH_3NH_3PbI_3$ perovskite solar cells reported to date ($E_g \sim 1.55\,\mathrm{eV}$), but higher bandgap materials are currently being investigated with various halide substitutions [23].

To simplify the optical analysis, additional carrier transport and electrode layers of the top cell are not included in the model, however carrier collection effects are included in the efficiency calculations in Sec. 5. We do not expect these layers to significantly change the optimum optical parameters of the SLARC and intermediate reflector layers, although the overall tandem cell performance may be reduced due to parasitic optical absorption. We also note that the present model does not include refractive index dispersion in the top cell and intermediate layers. Dispersion in thin films depends strongly on material and processing conditions and could be easily included in the optimization once specific materials were selected for each layer. However, this paper is not intended to identify specific materials, but rather to demonstrate a

#216827 - $15.00 USD Received 11 Jul 2014; revised 4 Aug 2014; accepted 17 Aug 2014; published 28 Aug 2014

general design concept for tandem solar cells. For this reason, we use typical refractive index values for the different layers, rather than detailed experimental dispersion data.

The bottom cell model is based on the 25% efficient c-Si PERL cell reported in [24, 25]. The response of this cell is calculated in two steps. First, the light transmitted through the top cell is calculated by including a semi-infinite Si substrate in the transfer matrix calculations described above. The transmitted spectrum is then combined with the measured external quantum efficiency (EQE) of the PERL cell [24, 26] to estimate the absorption and corresponding short circuit current. Thus, the bottom cell absorption curves shown in Fig. 2(a) are the experimental EQE curves modulated by the transmission spectrum of the top cell and intermediate layers.

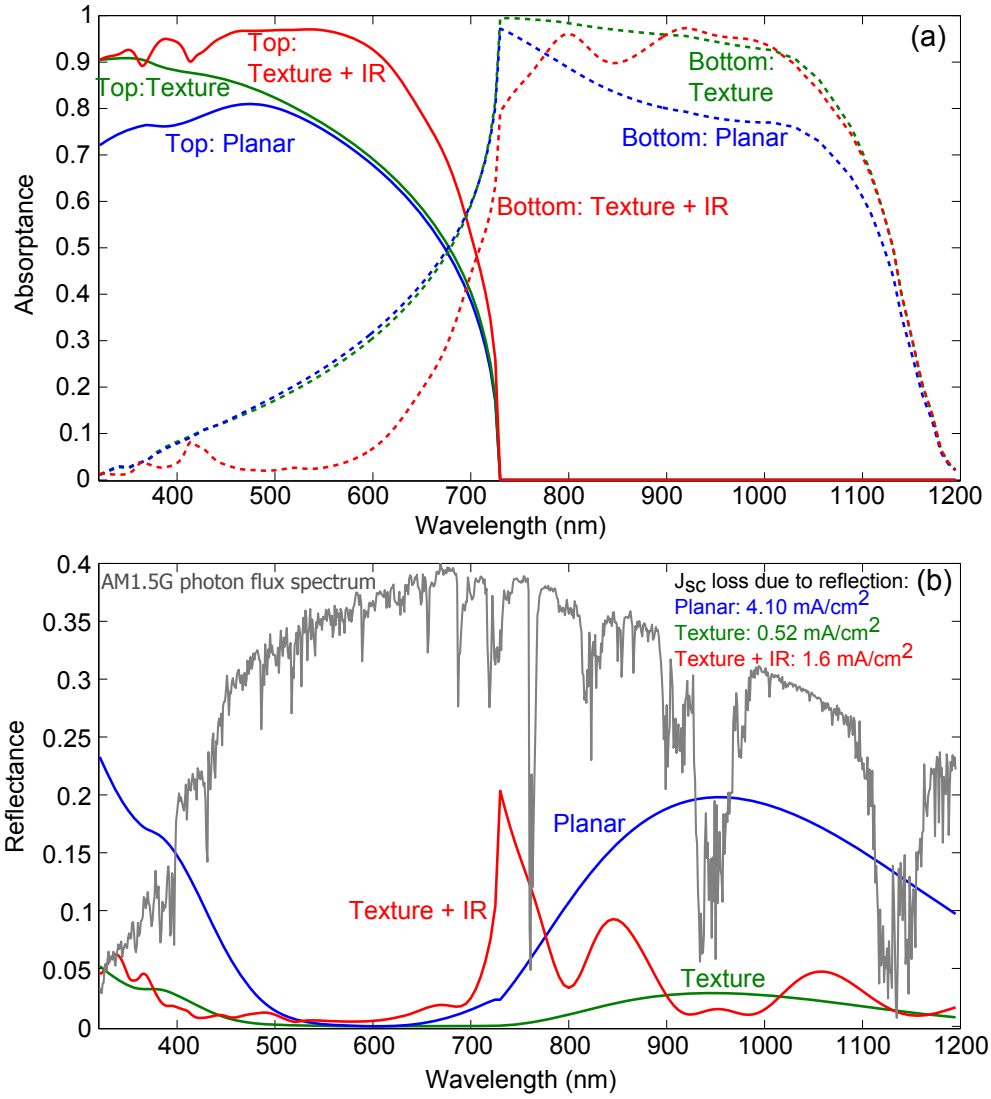

Fig. 2. Reflectance and absorptance in the top and bottom cells for various cell structures vs. wavelength. All structures have a thickness-optimized SLARC and top cell thickness of 150 nm. (a) Absorptance in top and bottom cells. (b) Front-surface reflectance and equivalent reflected J_{sc} values for each structure. A normalized AM1.5G solar spectrum is overlaid in gray for reference.

#216827 - $15.00 USD Received 11 Jul 2014; revised 4 Aug 2014; accepted 17 Aug 2014; published 28 Aug 2014

4. Results

As a reference case, we first consider an all-planar tandem cell with a SLARC on the front and no intermediate reflector. Throughout this paper the ARC film is taken to be a lossless dielectric with a refractive index of 1.7 (similar to Al_2O_3), with the thickness optimized to give the best tandem cell efficiency for each structure. The corresponding absorption and reflection spectra for a planar 150 nm thick perovskite top cell are plotted as blue curves in Fig. 2. Comparing the curves in Fig. 2(a) and 2(b) shows that the planar top cell suffers from reflection loss at short wavelengths ($\lambda < 500\,\text{nm}$), and weak absorption at wavelengths $500\,\text{nm} < \lambda < 730\,\text{nm}$ while the planar Si bottom cell suffers significant reflection losses at wavelengths $\lambda > 800\,\text{nm}$. The integrated reflection loss for the planar cell is equivalent to a short current loss of $4.1\,\text{mA}\,\text{cm}^{-2}$ under AM1.5G illumination.

To reduce the reflection losses, we next consider a textured cell structure as shown in Fig. 1, but without the intermediate reflector layer (green curves in Fig. 2). We assume that the front surface of the Si cell is patterned with inverted pyramids, and the thin top cell and optimized SLARC are deposited conformally over the surface. Pyramidal surface textures (upright and inverted) are commonly used on monocrystalline silicon cells for antireflection and light-trapping. The typical feature size is $2\,\mu\text{m} - 10\,\mu\text{m}$ and thus they can be modelled accurately using ray-optics [8]. Here we assume an inverted pyramid texture as illustrated in Fig. 1, but similar results would be expected for upright pyramids. In the ray optics regime there is no direct coupling of light between inverted pyramids, so random and regular arrays have the same optical response. We apply the semi-analytic approach of [8, 27], taking into account the multiple ray paths illustrated in Fig. 1(b). This method requires as inputs only the angle-dependent reflection and transmission coefficients of a single planar facet. Note that we correct the path proportions from those errantly reported in [8], so that 40% of incident light follows path B (Fig. 1(b)). As expected, the textured surface reduces the reflectance dramatically across the whole wavelength range of interest, resulting in an integrated reflection loss equivalent to $0.52\,\text{mA}\,\text{cm}^{-2}$ – almost eight times lower than the planar reference.

Despite the excellent anti-reflection provided by the surface texture, it offers no significant light trapping in the top cell. This can be seen by comparing the top cell absorption curves for the planar (blue) and textured (green) cells in Fig. 2(a). At wavelengths below 730 nm, absorption in the bottom cell is almost identical for the planar and simple textured cell structures, with $\sim 25\%$ of photons with energy $hc/\lambda > 1.7\,\text{eV}$ absorbed by the Si. Ideally, all such high-energy photons would be absorbed in the top cell to gain the maximum benefit of the larger bandgap. This requires wavelength-selective light trapping to increase absorption of short wavelength light in the top cell while transmitting long wavelength light to the bottom cell.

To provide light trapping in the top cell we next consider the addition of a wavelength-selective intermediate reflector (IR) between the top and bottom cells as shown in Fig. 1. The purpose of the IR is to prevent short wavelength light from entering the Si cell by reflecting it back through the top cell, as shown in Fig. 1(c). The path length enhancement in the top cell can therefore be up to a factor of four or six, depending on which of the ray paths in Fig. 1(b) the light follows. We choose a basic Bragg stack reflector consisting of alternating TiO_2 ($n_H = 2.4$) and SiO_2 ($n_L = 1.46$) layers with relative thicknesses fixed to maintain an equal optical path length in each material. A stack of four n_H/n_L layer pairs was chosen to ensure very high reflectance at the desired wavelengths, however we have found that fewer layers can provide relatively good light trapping, which may be desirable to simplify fabrication. Following the approach in [28], an additional thin (half-layer) SiO_2 film is included on the front and back of the stack to maximize coupling in and out of the IR layer, thereby minimizing reflectance at longer wavelengths.

Although it is straightforward to design a Bragg stack to achieve a reflectance band at a

#216827 - $15.00 USD Received 11 Jul 2014; revised 4 Aug 2014; accepted 17 Aug 2014; published 28 Aug 2014

specific wavelength for one angle of incidence, it is nontrivial to design one for the textured surface in Fig. 1, where light undergoes multiple reflections. The design process is further complicated by the requirement to minimize reflectance for longer wavelengths. For this reason we perform a simple numerical optimization of the IR layer thickness and the SLARC thickness in order to maximize the overall tandem efficiency (calculated as in Sec. 5). The optimization is repeated for each top cell thickness.

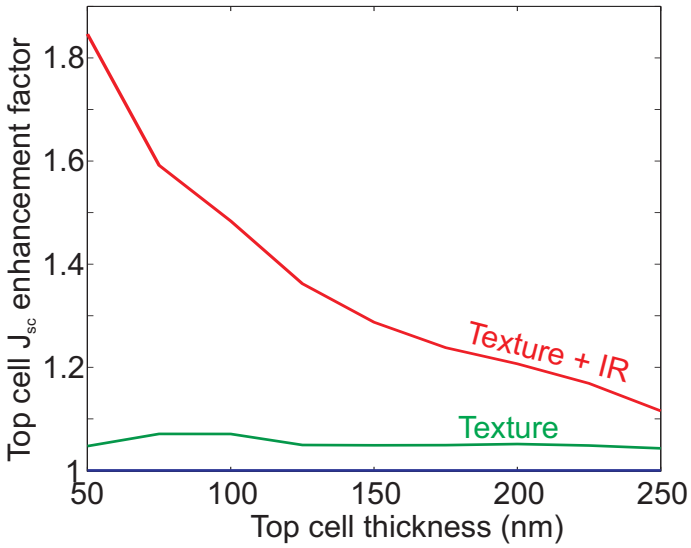

Fig. 3. J_{sc} enhancement factor for each cell structure vs. top cell thickness. This factor is the ratio of the top cell J_{sc} of a given structure to the J_{sc} of the planar cell at equal top cell thickness

The red curves in Fig. 2(a) show the absorptance in the top and bottom cells with the optimized texture/IR combination for a 150 nm thick top cell. The corresponding reflectance spectrum is plotted in Fig. 2(b). Light trapping of short wavelength light is evident by the increased absorption in the top cell and corresponding decrease in absorption in the bottom cell. Less than 12% of photons with energy $hc/\lambda > 1.7$ eV are absorbed in the bottom cell, while the overall reflectance remains $< 5\%$ at these wavelengths. Figure 2(b) shows a slight increase in reflectance with the addition of the IR layer, resulting in an integrated reflection loss of $1.6\,\mathrm{mA\,cm^{-2}}$. Most of this increase is due to imperfect transmission of long wavelength light through the IR layer, which could perhaps be improved with a more complex IR design.

Figure 3 shows the relative current enhancement in the top cell as a function of its thickness for the texture-only and texture/IR cases, normalized to the planar reference structure. The texturing alone achieves a current increase of $\approx 5\%$ for all top cell thicknesses, indicating reduced reflectance, but little light trapping. In contrast, adding the wavelength-selective IR layer between the cells increases current in the top cell by $> 80\%$ for a 50 nm thick top cell, and $\sim 11\%$ for a 250 nm thick cell. The large enhancement for thin films, and strong dependence on cell thickness is characteristic of effective light trapping in the top cell. Thus, the proposed tandem cell geometry in Fig. 1 successfully combines the excellent broadband anti-reflection properties of conventional pyramidal surface texturing with wavelength-selective light trapping in the thin-film top cell.

Although the results presented so far demonstrate reduced reflectance and improved light trapping in the top cell, further analysis is required to understand the potential efficiency gains

#216827 - $15.00 USD Received 11 Jul 2014; revised 4 Aug 2014; accepted 17 Aug 2014; published 28 Aug 2014

offered by this approach. In the next section we use a simple tandem cell efficiency model reported in [6] to estimate the overall tandem cell efficiency.

5. Tandem cell efficiency

In this section we follow the approach described in [6] to calculate the efficiency of a 4-terminal tandem cell using the calculated absoption spectra in Fig. 2. In this model, the carrier collection and voltage properties of the top cell depend on the cell thickness, and are characterized by the bandgap ($E_{g,top} = 1.7\,\mathrm{eV}$), carrier diffusion length ($L_d = 110\,\mathrm{nm}$), and luminescence efficiency $\Phi = 0.55$ of the absorbing layer. The chosen values of L_d and Φ are based on experimentally-determined values for solution-processed perovskite films reported in [4] and [29] respectively. As in [6], here we assume the top cell has a fill-factor of 0.8, which, while higher than current perovskite cells, is a realistic target for future high efficiency devices.

Carrier collection in the Si bottom cell is already accounted for in the absorption data (Fig. 2) where we used the experimental EQE curves for a high efficiency PERL cell, as described in Sec. 3. A simple one-diode model is then used to calculate the V_{oc} of the bottom cell as a function of the calculated J_{sc}. We assume that the fill-factor and J_0 are unchanged from their values under standard test conditions.

With the above models for the top and bottom cell performance, the total output power of the 4-terminal device is given by $P = FF^{(1)}V_{oc}^{(1)}J_{sc}^{(1)} + FF^{(2)}V_{oc}^{(2)}J_{sc}^{(2)}$, where the superscripts 1 and 2 denote the top cell and bottom cell respectively [6].

Figure 4 shows the short circuit current density in the top and bottom cells (a) and the calculated tandem cell efficiency (b) as a function of top cell thickness for the three cases studied here: the planar reference cell; the textured cell; and the textured cell with intermediate reflector. As seen in Fig. 4(a), the surface texture provides an almost fixed increase in the top cell J_{sc} of $\sim 5\%$, and a relatively larger increase in the bottom cell J_{sc}, resulting in an absolute efficiency increase of $\sim 2\%$ for most cell thicknesses (Fig. 4(b)). Comparing the reflectance curves in Fig. 2(b) for the planar and textured cases, it is clear that this increase is largely due to reduced front surface reflectance at wavelengths above 730 nm.

Despite a small increase in reflection loss ($\sim 1.1\,\mathrm{mA\,cm^{-2}}$), the addition of the IR achieves further absolute efficiency gains of $1-2\%$ above those of the basic textured cell, and $2-4\%$ above the planar reference cell. This is due to the large top cell J_{sc} enhancement resulting from effective light-trapping of short wavelength light (Fig. 2). This transfer of current to the top cell results in a net efficiency gain due to its higher V_{oc}.

Figure 4(b) also shows the efficiency beginning to saturate for top cell thicknesses of 250 nm for the optimized texture + IR structure. This is a result of almost complete absorption of above-bandgap light in the top cell. Further increase in cell thickness eventually results in decreasing current and overall efficiency due to reduced collection efficiency (noting that the carrier diffusion length considered here was 110 nm).

Light trapping also has the effect of bringing the top and bottom J_{sc} values closer to each other: the difference between top and bottom J_{sc} for the cell with the IR is $< 5\,\mathrm{mA\,cm^{-2}}$ for a 150 nm thick top cell, compared to $> 12\,\mathrm{mA\,cm^{-2}}$ for the simple textured cell (see Fig. 4(a)). Hence, the light trapping scheme proposed here could also provide effective photon management in series connected cells where current-matching is required.

6. Conclusion

We present a practical tandem cell structure combining conventional pyramidal surface texturing on the Si bottom cell with a wavelength-selective intermediate reflector. This design satisfies the three optical requirements for high-performance perovskite-on-silicon tandem solar cells: low front surface reflectance, light-trapping of short wavelength light, and high transmission of

#216827 - $15.00 USD Received 11 Jul 2014; revised 4 Aug 2014; accepted 17 Aug 2014; published 28 Aug 2014

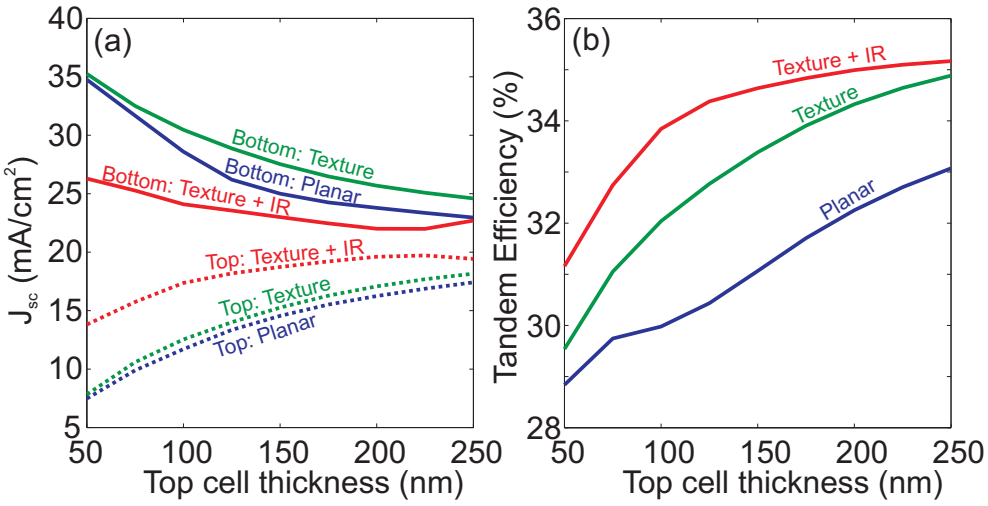

Fig. 4. (a) Jsc for top and bottom cells for each structure vs. top cell thickness. (b) Efficiency of each structure vs. top cell thickness.

long wavelength light to the bottom cell. We calculate front-surface reflection losses as low as $1.6\,\mathrm{mA\,cm^{-2}}$, and top cell current enhancements of $>80\%$ for a 50 nm thick perovskite top cell, and $>20\%$ for a 200 nm top cell. This performance corresponds to absolute efficiency increases of $2-4\%$ compared to a planar tandem cell with a single layer ARC on the front surface. Using a simple tandem cell efficiency model, we have shown that efficiencies as high as 35% may be achievable with an optimal high-bandgap perovskite top cell.

While the concept has been demonstrated for a specific tandem cell combination, it is applicable to any thin-film on Si tandem cell provided a high quality top cell can be fabricated conformally on the textured bottom cell. This has been recently demonstrated for a-Si cells [12], and is well-suited to evaporated perovskite cells [5]. We would also expect similar performance enhancements on other Si surface textures such as upright and random pyramids.

This work shows that existing high-efficiency front-surface textured c-Si cell designs offer an ideal substrate to deposit a thin film top cell. The approach is therefore directly compatible with mechanically-stacked tandem cells with little or no modification to the Si cell manufacturing process, and is therefore highly attractive for rapid development of silicon-based tandems. Such integrated light trapping will also be important for series-connected tandem cells where high absorption in the top cell is crucial for current matching requirements.

Acknowledgment

N.N.L is supported by an Australian Renewable Energy Agency (ARENA) postdoctoral fellowship.

#216827 - $15.00 USD Received 11 Jul 2014; revised 4 Aug 2014; accepted 17 Aug 2014; published 28 Aug 2014